

# NEDD4L Regulates the Proliferation and Metastasis of Non-small-cell Lung Cancer by Mediating CPNE1 Ubiquitination

**Ruochen Zhang**

Institute of Respiratory Diseases, soochow University

**Yuanyuan Zeng**

Institute of Respiratory Diseases, Soochow University.

**Weijie Zhang**

Soochow University

**Yue Li**

Soochow University

**Jieqi Zhou**

Soochow University

**Yang Zhang**

Soochow University

**Anqi Wang**

Soochow University

**Yantian Lv**

Soochow University

**Jianjie Zhu**

First Affiliated Hospital of Soochow University

**Zeyi Liu** (✉ [liuzeyisuda@163.com](mailto:liuzeyisuda@163.com))

First Affiliated Hospital of Soochow University <https://orcid.org/0000-0003-2528-6909>

**Jian-an Huang**

First Affiliated Hospital of Soochow University

---

## Research

**Keywords:** NSCLC, CPNE1, NEDD4L, ubiquitination, degradation

**Posted Date:** February 26th, 2021

**DOI:** <https://doi.org/10.21203/rs.3.rs-250598/v1>

**License:** © ⓘ This work is licensed under a Creative Commons Attribution 4.0 International License. [Read Full License](#)

---

# Abstract

High expression of CPNE1 is positively correlated with the occurrence, TNM stage, lymph node metastasis, and distant metastasis of non-small-cell lung cancer (NSCLC), suggesting that CPNE1 may be an effective target for the treatment of NSCLC. No direct role of post-translational modification of CPNE1 in NSCLC has been reported. This study confirms that CPNE1 is degraded by two pathways: the ubiquitin-proteasome pathway and the autophagy-lysosome pathway. CPNE1 binds with the ubiquitin molecule via its K157 residue. Moreover, we determine that the ubiquitin ligase NEDD4L can mediate the ubiquitination of CPNE1 and promote its degradation. In addition, we find that NEDD4L knockout promotes the proliferation and metastasis of NSCLC cells by regulating CPNE1. This study aims to further investigate the mechanism of CPNE1 ubiquitination in the occurrence and development of NSCLC and provide a new potential target for NSCLC treatment.

## Introduction

Lung cancer is the leading cause of death from malignancies worldwide [1]. NSCLC is characterized by difficulty in surgical resection, a tendency toward postoperative metastasis and recurrence, and insensitivity to radiotherapy and chemotherapy [2]. Traditional treatment regimens are not easy to undergo, which causes great distress to patients with non-small-cell lung cancer. In the past two decades, significant advances have been made in the treatment of NSCLC that have improved our understanding of the biology and pathogenesis of tumor disease. The use of small molecule tyrosine kinase inhibitors and immunotherapy can increase the survival benefit in lung cancer patients, but drug resistance is a problem in some patients after treatment [3, 4]. Currently, the overall cure and survival rates of NSCLC remain low. Therefore, it is of great importance to further study the specific molecular mechanism underlying the occurrence and development of lung cancer, search for new drug targets, reduce the mortality rate and improve the prognosis of NSCLC patients.

Copine (CPNE) proteins, members of a family of calcium-dependent phospholipid-binding proteins, are highly conserved with high sequence similarity. They are widely distributed from plants to humans [5, 6]. The CPNE family contains nine members (CPNE1 to CPNE9), all of which have 2 tandem C2 domains (C2A and C2B) at the N-terminus and an A domain at the C-terminus [7]. The C2 domains, which have been originally identified in protein kinase C [8], are thought to play important roles in signal transduction and membrane trafficking [9]. The A-domain, named for von Willebrand factor, a plasma and extracellular matrix protein, has been studied in integrins and several extracellular matrix proteins and appears to function as a protein-binding domain [8, 10]. This family of proteins regulates multiple biological functions, including cell proliferation, migration, and differentiation [11–13].

In the present study, high expression of CPNE1 was correlated with poor prognosis and clinical progression in various cancers. Evidence implies that high CPNE1 expression might be an independent prognostic indicator of poor recurrence-free survival in prostate cancer [14]. In addition, knockdown of CPNE1 inhibits osteosarcoma progression by downregulating the expression of Ras, MEK-1/2, WNT1,  $\beta$ -catenin, cyclin A1, IRAK2, and cIAP2 [15]. In triple-negative breast cancer, CPNE1 induces tumorigenesis and radio resistance by activating the AKT pathway [16]. Moreover, 14-3-3 $\gamma$  and Jab1 induce CPNE1-mediated neuronal differentiation by directly binding to CPNE1 [17, 18]; conversely, HAX1 has an opposing effect [19]. Our previous study found that high expression of CPNE1 was positively correlated with TNM stage, lymph node metastasis, and distant metastasis in 128 lung cancer tissues. In addition, miR-335-5p was shown to downregulate the proliferation and migration of lung cancer cells by directly targeting the CPNE1 3'-UTR [20]. And miR-195-5p was responsible for the ability of high CPNE1 expression to induce poor prognosis in squamous cell lung cancer (SCC) and lung adenocarcinoma (ADC) [21].

Neural precursor cell expressed developmentally downregulated 4-like(NEDD4L) is a member of the NEDD4 family and contains a C2 domain for membrane binding, a HECT domain for Ub protein ligation, and a central region including 4 WW domains for substrate recognition [22, 23]. NEDD4L was downregulated in NSCLCs. This downregulation correlated with lymph node invasion, advanced stage and poor survival [24]. As a ubiquitin ligase, NEDD4L specifically identifies a TGF- $\beta$ -induced phospho-Thr-Pro-Tyr motif, inducing Smad2/3 polyubiquitination and degradation [25, 26].

In melanoma, NEDD4L is activated by p-MEK1/2 and ubiquitinates SP1 at the K685 residue, which leads to proteasomal degradation of SP1 [27]. NEDD4L acts as a tumor suppressor gene and is downregulated in lung cancer, indicating that it has a role in the initiation and progression of lung cancer [24, 28].

Although regulation of CPNE1 at the post-translational level has been extensively studied, little is known about the mechanisms of CPNE1 regulation at the transcriptional and translational levels. In the present study, we explored CPNE1 degradation via the ubiquitin-proteasome pathway and revealed that NEDD4L directly interacted with CPNE1 as a ubiquitin ligase. Furthermore, the underlying mechanism was elucidated.

## Materials And Methods

### Tissue samples

Paired NSCLC and adjacent noncancerous lung tissue samples were collected with the informed consent of patients from the First Affiliated Hospital of Soochow University. The patients had been diagnosed with NSCLC based on their histological and pathological characteristics according to the revised International System for Staging Lung Cancer. They had not undergone chemotherapy or radiotherapy before tissue sampling. The tissue samples were snap frozen and stored in a cryogenic freezer at  $-80^{\circ}\text{C}$ . This study was approved by the Academic Advisory Board of Soochow University.

### Cell culture

The human NSCLC cell lines A549, H1299, SPC-A1, and HCC827 and HEK293T cells were purchased from the Cell Bank of the Chinese Academy of Sciences (Shanghai, China). Cells were cultured in RPMI 1640 medium and DMEM supplemented with 10% foetal bovine serum (Gibco, Carlsbad, CA, USA) and L-glutamine (Invitrogen, Carlsbad, CA, USA) under standard cell culture conditions (5 %  $\text{CO}_2/37^{\circ}\text{C}$ ).

### Immunohistochemical (IHC) assay

Immunohistochemical assays were performed as previously described<sup>29</sup>. In brief, slides were incubated with an anti-CPNE1 antibody (diluted 1:100; Abcam, shanghai, China) and an anti-NEDD4L antibody (diluted 1:100; Abcam, shanghai, China) overnight at  $4^{\circ}\text{C}$  and were then incubated with the corresponding biotinylated secondary antibodies. Immunoreactions were visualized using a DAB kit (BD Biosciences, San Jose, CA, USA). Briefly, the proportion score was graded as follows: staining in 0% of the cells examined was counted as 0; 0.01%–25% was counted as 1; 25.01%–50% was counted as 2; 50.01%–75% was counted as 3; and 75%-100% was counted as 4. The staining intensity was graded as follows: 0, no signal; 1, weak; 2, moderate; and 3, strong. The histological score for each section was computed using the formula: histological score = proportion score  $\times$  intensity score. A total score in the range of 0–12 was calculated and graded as follows: negative (-, score: 0), weak (+, score: 1–4), moderate (++, score: 5–8) or strong (+++, score: 9–12).

## **Plasmid construction and mutagenesis.**

The CDS region of CPNE1 was amplified using cDNA from H1299 cells as the template and was cloned into FLAG-PCDH. For mutagenesis, Flag-CPNE1 was used as the template for PCR amplification. Amplification products were mixed with 2 µl of buffer and 1 µl of DpnI restriction enzyme and incubated at 37 °C for 3 h. Then, the mixture was used for bacterial transformation, and sequencing was then conducted at Suzhou GENEWIZ Biotechnology. The primer sequences used for the construction of Flag-CPNE1 and mutagenesis are shown in Supplementary Table S2.

## **Protein stability assays**

CHX, an inhibitor of protein synthesis, was used to determine the half-life of CPNE1. Cells were treated with CHX (100 µg/ml) for 2, 4, 6, 8, and 10 h separately before protein extraction. CPNE1 degradation was analysed by Western blotting.

## **RNA interference**

Two pre-designed small interfering RNA (siRNA) sequences corresponding to the target sequences were directly synthesized (GenePharma). The siRNA constructs are described as follows: siRNA-NEDD4L-1: 5'-GAGTACCTATGAATGGATT-3'(sense) and 5'-AATCCATTC ATAGGTACTC-3'(antisense); siRNA-NEDD4L-2: 5'-CAGAAATAATGGTCACAAA-3'(sense) and 5'-TTTGTGACCATTATTTCTG-3' (antisense); siRNA-CPNE1-1: 5'-GCAGGUCUCGCAU GAAUUUTT-3'(sense) and 5'-AAAUUCAUGCGAGACCUGCTT-3'(antisense). Transfection of siRNA into cells was performed with Lipofectamine 2000 according to the instructions of the manufacturer.

## **Western blot analysis and co-immunoprecipitation assay**

Western blotting (WB) was performed as previously described [29]. The antibodies used for the analysis were anti-CPNE1 (Abcam, Shanghai, China) and anti-NEDD4L (CST, UK). For co-immunoprecipitation experiments,  $2 \times 10^5$  HEK293T cells were transfected with the required plasmids for 48 h. Cells were harvested with 1 ml of RIPA buffer. Equal amounts of protein were incubated with 2 µg of M2 anti-Flag affinity agarose at 4 °C for 4 h with end-over-end rotation. The protein-antibody complexes were collected by centrifugation and washed 3 times with RIPA buffer. Then, the precipitates were analysed by Western blotting.

## **Immunofluorescence**

In brief, cells were fixed with 4% formaldehyde for 15 min and blocked with 5% BSA for 30 min. Then, the cell climbing slices were incubated overnight with a rat anti-NEDD4L antibody (1:100; CST, UK) and a mouse anti-CPNE1 antibody (1:100; Santa, Temecula, CA). After washing with PBS three times, the cell climbing slices were incubated with a fluorescent secondary antibody at room temperature for 1 h. Nuclei were then stained with DAPI. Finally, the slices were observed and images were acquired under a confocal microscope.

## **Cell proliferation analysis**

Cell proliferation was evaluated using CCK-8 assays. Cells were digested and plated at a concentration of  $3 \times 10^3$  cells per well in 96-well plates under standard cell culture conditions. A Cell Counting Kit-8 (Boster, Wuhan, China) was used to detect cell proliferation after culture for 24, 48, and 72 h.

## **Colony Formation Assay**

A colony formation assay was used to confirm malignant transformation. Three thousand cells were seeded in 3ml of RPMI 1640 medium supplemented with 10% foetal bovine serum and incubated at 37 °C with 5% CO<sup>2</sup>. The number of colonies formed after 14 days was counted using ImageJ.

### **Migration and invasion assays**

Cell motility was assayed using 12-well transwell plates (Corning) as described before [28]. Experiments were performed in 24-well transwell plates with 8-µm pore-size chambers. The difference between the cell migration and invasion assays was whether the top surface of the filter was pre-coated with Matrigel. In brief, lung cancer cells (5× 10<sup>4</sup>) were plated in the upper compartment of the transwell chamber in medium containing 1% FBS. Then, 0.8ml of complete medium was added to the lower compartment of the chamber. Cells on the upper surface of the filter were removed after 24 hours in both the migration and invasion assays. Images were acquired using a microscope (CKX41, Olympus)

### **Statistical analysis**

We used Student's t-test (two-tailed) and two-way ANOVA to analyse the results when required. P<0.05 indicates that difference between groups was significant. All data were analysed using GraphPad Prism 8.

## **Results**

### **1. CPNE1 is elevated in lung cancer and correlates with poor survival**

We first investigated the possible role of CPNE1 by analysing data in a publicly available database. We detected in the TCGA database that CPNE1 is upregulated in a variety of cancers (<https://portal.gdc.cancer.gov>) (Fig. 1a). By performing differential analysis of pan-cancer expression data obtained from the OSLuca database (<http://bioinfo.henu.edu.cn/LUCA/LUCAList.jsp>) [30], we found that CPNE1 is an oncogene (Fig. 1b). Then, analysis of the starBase database (<http://starbase.sysu.edu.cn/index.php>) showed that CPNE1 was highly expressed in 501 lung adenocarcinomas compared with 49 normal tissues (Fig. 1c). Consistent upregulation of CPNE1 expression was also observed in lung squamous cell carcinoma (Fig. 1d). In addition, high expression of CPNE1 was related to the TNM stage of patients with lung adenocarcinoma and lung squamous cell carcinoma (<https://ccsm.uth.edu/miRacDB>) (Fig. 1e, f). Analysis of survival data showed that CPNE1 correlated with poor survival in lung cancer patients (<http://bioinfo.henu.edu.cn/LUCA/LUCAList.jsp>) (Fig. 1g, h, i).

### **2. CPNE1 is degraded through both the ubiquitin-proteasome pathway and the autophagy-lysosome pathway.**

We found that the expression of CPNE1 in lung cancer cell lines (A549, H226, H1299, H1650, SPC-A1, HCC827, and H460) was higher than that in a normal lung epithelial cell line (BEAS-2B) using Western blotting (Fig. 2a); This result was consistent with previous conclusions obtained by database analysis. We next measured CPNE1 degradation rates by a cycloheximide (CHX) chase assay. As shown in Fig. 2b, CHX treatment led to CPNE1 protein degradation in a time-dependent manner in HEK293T cells. In addition, the CPNE1 protein level was significantly reduced after CHX treatment for 2 h (Fig. 2c). This result confirms that the CPNE1 protein is unstable, suggesting that analysing of the mechanism of CPNE1 protein degradation is of great importance for the functional study of CPNE1. To determine whether this degradation involves the proteasome pathway, we treated lung cancer cells with CHX alone or with both CHX and MG132 to inhibit proteasomal degradation (Fig. 2d). In the absence of MG132, CPNE1 was obviously degraded, while proteasome inhibition by MG132 reversed this degradation, notably

stabilizing CPNE1. The above results indicated that degradation of the CPNE1 protein occurred through a proteasome-mediated ubiquitination degradation pathway. Interestingly, to further investigate the degradation of the CPNE1 protein, we evaluated the degradation of endogenous CPNE1 through the lysosomal pathway and the proteasome pathway. The results showed that when MG132 or 3-MA was added, endogenous CPNE1 protein accumulated (Fig. 2e, f). Taken together, these results confirm that the CPNE1 protein is degraded by both the ubiquitin-proteasome pathway and the lysosomal pathway in lung cancer cells.

### 3. CPNE1 undergoes ubiquitination, and a highly conserved lysine at position 157 is subjected to ubiquitination.

To gain further insight into the mechanism of CPNE1 degradation, we evaluated whether CPNE1 is conjugated with Ub *in vivo*. Ubiquitin (Ub) and Flag-CPNE1 plasmids were co-transformed into HEK293T cells. The results showed obvious ubiquitin bands, and MG132 strengthened the ubiquitin bands (Fig. 3a). Generally, there are three types of ubiquitination modification of substrate proteins: a single ubiquitin molecule labelling a single lysine site (single monoubiquitination), multiple ubiquitin molecules labelling a single lysine site (poly monoubiquitination), and ubiquitin chains labelling multiple different lysine residues (polyubiquitination) [31]. If a particular protein has been extensively polyubiquitinated before it is recognized by the proteasome, then the application of lysine-less ubiquitin (UB-K0) will reduce proteolysis [32]. As shown in Fig. 3b, co-expression with UB-K0 resulted in an increase of more than 1.35-fold in CPNE1 protein levels, indicating extensive polyubiquitination prior to CPNE1 degradation by the proteasome. To further identify the specific lysine residues of CPNE1 to which the ubiquitination chain is conjugated, we input the CPNE1 protein sequence from the NCBI database into different ubiquitin site prediction software programs (Table 1). K60, K84, K120, K135, K157, K190, K522, and K529 are the most likely ubiquitinated lysine residues, as predicted by several prediction websites (Supplementary Fig. 1). Then, we generated a set of CPNE1 mutants by substituting individual lysine (K) residues with arginine (R) residues. We found that the CPNE1 K157R mutant had a lower level of ubiquitination than WT CPNE1 (Fig. 3c). CPNE1 protein sequences of different species were downloaded from the NCBI database, and the CPNE1 K157 residue was found to be conserved across those species (Fig. 3d). Collectively, these results indicate that K157 is a major ubiquitination site of CPNE1.

Table 1  
Prediction of CPNE1 ubiquitination sites

Positions of predicted sites	Prediction tool	Web address of prediction tool
20,60,117,120,151,152,248,252,253,256,264,522,529	BDM-PUB	<a href="http://bdmpub.biocuckoo.org/result.php">http://bdmpub.biocuckoo.org/result.php</a>
60,73,84,135,157,182,190,522,529	UbiBrowser	<a href="http://ubibrowser.ncpsb.org">http://ubibrowser.ncpsb.org</a>
20,25,60,73,84,117,120,135,151,152,157,171,182,190, 248,251,252,253,256,264,334,522,529	UbPred	<a href="http://www.ubpred.org/">http://www.ubpred.org/</a>
25,84,120,135,157,190	UbiProber	<a href="http://bioinfo.ncu.edu.cn/ubiprober.aspx">http://bioinfo.ncu.edu.cn/ubiprober.aspx</a>

### 4. NEDD4L was identified as ubiquitin ligase for CPNE1

E3 ligases often determine the specificity of ubiquitin-proteasome protein degradation. We next sought to identify the E3 ubiquitin ligase that targets CPNE1. NEDD4L was identified as the E3 ligase of CPNE1 via UbiBrowser (Fig. 4a). NEDD4L expression is downregulated in multiple types of human cancers (<https://portal.gdc.cancer.gov>) (Fig. 4b), suggesting that NEDD4L expression levels are downregulated in human lung cancer tissues and correlate

with poor prognosis in lung cancer, in turn suggesting that NEDD4L deficiency may promote cancer cell invasion during malignant progression (<http://bioinfo.henu.edu.cn/LUCA/LUCAList.jsp>) (Fig. 4c). We sought to evaluate NEDD4L expression levels in humans. The protein levels of NEDD4L were detected by immunohistochemical staining. High NEDD4L expression in 8 tumour specimens and 4 adjacent non-tumour specimens (Fig. 4d). The results shown in Fig. 4e (<http://gepia2.cancer-pku.cn>) and Fig. 4f (<https://cistrome.shinyapps.io/timer/>) confirm that there is no correlation between CPNE1 and NEDD4L at the mRNA level. We evaluated the expression levels of CPNE1 and NEDD4L in lung tissues (tumor specimens and adjacent non-tumor specimens) by Western blotting. Among 14 paired cancer tissues, negative or low protein expression of CPNE1 was detected in 4 samples (Fig. 4g, Supplementary Table S1), and high expression was detected in 10 samples, while 57% were negative for NEDD4L expression and the rest were positive. There was a negative correlation between CPNE1 and NEDD4L at the protein level (Fig. 4h), which revealed that the interaction between these proteins occurs at the post-translational level. Taken together, these results indicate that NEDD4L plays a critical role in negative regulation of CPNE1.

## 5. NEDD4L interacts with the CPNE1 protein.

To investigate the interaction between CPNE1 and NEDD4L, we performed a co-immunoprecipitation (co-IP) assay. CPNE1 co-immunoprecipitated with NEDD4L in A549, H1299 and SPC-A1 cells (Fig. 5a). We further investigated the localization of CPNE1 and NEDD4L in lung cancer cells. Immunostaining showed that NEDD4L was mainly localized in the cytosol, while CPNE1 was localized in both the cytosol and the nucleus (Fig. 5b). Next, we verified the regulatory effect of NEDD4L on CPNE1. NEDD4L downregulation increased CPNE1 protein expression (Fig. 5c). Interestingly, this increase was strongly suppressed by MG132, suggesting that the regulation of CPNE1 by NEDD4L is mediated via the ubiquitin-proteasome pathway (Fig. 5d).

## 6. NEDD4L knockout promotes tumor cell proliferation and metastasis through CPNE1

To further characterize the regulation of NEDD4L-induced CPNE1 upregulation in lung cancer cells, we established stable NEDD4L knockout (NEDD4L KO) A549 cell lines (Fig. 6a). NEDD4L-KO enhanced the proliferation of A549 cells, whereas CPNE1 interference reversed this facilitatory effect (Fig. 6b, c). Subsequently, the proportion of NEDD4L-KO cells in G0/G1 phase and the proportion of NEDD4L-KO cells in S phase were significantly lower and higher, respectively, than the corresponding proportions of control cells. Similarly, this effect was inhibited by interference with CPNE1 expression (Fig. 6d). Transwell migration and invasion assays showed that NEDD4L knockout promoted lung cancer cell migration and invasion. Furthermore, the migration and invasion abilities were restored by CPNE1 interference (Fig. 6e). In conclusion, the regulatory activity of NEDD4L on CPNE1 can affect the biological function of CPNE1.

## Discussion

Our previous studies confirmed that CPNE1 plays an important role in the development of cancer. CPNE1 was highly expressed in lung cancer and was positively correlated with TNM stage and lymph node metastasis. Overexpression of CPNE1 can activate Src, FAK, AKT, ERK, and other signalling pathways *in vivo* and promote the proliferation and metastasis of lung cancer cells. To elucidate the specific mechanism of the high expression of CPNE1 in lung cancer, we studied its regulation at the pre-transcriptional level. We found that miR-335-5p inhibited the expression of CPNE1 by directly targeting the CPNE1 3'-UTR, thus inhibiting the proliferation and invasion of NSCLC cells. In addition, miR-195-5p is responsible for the ability of high CPNE1 expression to result in poor prognosis in squamous cell lung cancer (SCC) and lung adenocarcinoma (ADC).

This study was the first to investigate the mechanism of CPNE1 degradation. We demonstrated that CPNE1 can be degraded by both the ubiquitin-proteasome and lysosomal proteolysis pathways. This study mainly focused on the degradation of CPNE1 via the ubiquitin-proteasome pathway. First, we confirmed that CPNE1 can interact with ubiquitin and that the CPNE1-K157 residue played a significant role in this interaction. Second, we identified NEDD4L as a ubiquitin ligase for CPNE1. NEDD4L knockout stabilized the CPNE1 protein and enhanced the proliferation and metastasis of lung cancer cells. In addition, the effect of NEDD4L was reversed by CPNE1 interference (Fig. 7). Additional studies are needed to further validate our hypothesis. The K157 residue of CPNE1 is essential for the ubiquitination of CPNE1, but whether it can affect the biological function of CPNE1 by affecting the ubiquitination of CPNE1 needs further study. Residues subject to polyubiquitination modification include K6, K11, K27, K29, K33, K48, and K63. Polyubiquitination at K11 and K48 mainly plays a role in protein degradation and the regulation of protein stability. Modification of K63 mainly affects signal transduction, DNA repair, and regulation of protein activity. Modification of K6 is related to mitosis [33]. It is important to determine the amino acid residues involved in the interaction between Ub and CPNE1. In addition, the mechanism by which NEDD4L regulates CPNE1 remains to be elucidated. For example, the domain via which CPNE1 and NEDD4L interact is unknown.

## Conclusion

Our study is the first to report the specific mechanism of CPNE1 degradation and showed that NEDD4L is responsible for CPNE1 degradation by the ubiquitin-proteasome pathway. NEDD4L KO can stabilize the CPNE1 protein and inhibit the proliferation and metastasis of NSCLC cells. In addition, we found that CPNE1 interacted with Ub via its K157 residue. Therefore, our findings further reveal the specific mechanism of CPNE1 in NSCLC carcinogenesis. The discovery of this NEDD4L-mediated ubiquitination of CPNE1 provides new insight into therapeutic strategies for NSCLC.

## Abbreviations

NSCLC: Non-small cell lung cancer; SCC: squamous cell lung cancer; ADC: lung adenocarcinoma; Ub: Ubiquitin; NEDD4L: Neural precursor cell expressed developmentally downregulated 4-like; NEDD4L KO: NEDD4L Knockout; CHX: Cycloheximide; miRNA: miRNA;

## Declarations

### Acknowledgements

We thank all patients who participated in this study for their cooperation, and we thank Dr Jun Chen and Dr Hua-Long Qin at The First Affiliated Hospital of Soochow University, Suzhou, China, for clinical sample collection.

### Authors' contributions

RCZ, YYZ, WJZ were responsible for doing the experiments, acquisition of data, and analysis and drafted the manuscript. YL, JQZ, and YTL provided and collected the clinical data. AQW and YZ and JJZ participated in the revising of the manuscript. JAH and ZYL were responsible for designing the experiments and supervising the study. All authors read and approved the final manuscript.

### Founding

This work was supported by grants from the National Natural Science Foundation of China (82073213 and 81802885), Jiangsu Provincial Medical Youth Talent (No. QNRC2016746), Gusu Youth Health Talent of Suzhou (No. 2020-082), Science and Technology Plan Project of Suzhou (No.SYS2020008), The Science and Technology Development Projects of Suzhou (No. SZYJTD201801), Suzhou Key Laboratory for Respiratory Medicine (No. SZS201617), and Jiangsu Provincial Key Medical Discipline (No. ZDXKB2016007).

### **Availability of data and materials**

The datasets generated and analysed during the current study are not publicly available because that it also forms part of another ongoing study, but are available from the corresponding author on reasonable request.

### **Ethics approval and consent to participate**

This study was approved by the Academic Advisory Board of Soochow University. All subjects involved were well informed.

### **Consent for publication**

Not applicable

### **Competing interests**

The authors have no conflicts of interest.

## **References**

1. Bray F, Ferlay J, Soerjomataram I, Siegel R, Torre L, Jemal A. Global cancer statistics 2018: GLOBOCAN estimates of incidence and mortality worldwide for 36 cancers in 185 countries. *CA: a cancer journal for clinicians*. 2018;68(6):394-424.
2. Pilkington G, Boland A, Brown T, Oyee J, Bagust A, Dickson R. A systematic review of the clinical effectiveness of first-line chemotherapy for adult patients with locally advanced or metastatic non-small cell lung cancer. *Thorax*. 2015;70(4):359-67.
3. Park S, Lee M, Seong M, Kim S, Kang J, Cho B, et al. A phase II, multicenter, two cohort study of 160 mg osimertinib in EGFR T790M-positive non-small-cell lung cancer patients with brain metastases or leptomeningeal disease who progressed on prior EGFR TKI therapy. *Annals of oncology : official journal of the European Society for Medical Oncology*. 2020;31(10):1397-404.
4. Soria J, Ohe Y, Vansteenkiste J, Reungwetwattana T, Chewaskulyong B, Lee K, et al. Osimertinib in Untreated EGFR-Mutated Advanced Non-Small-Cell Lung Cancer. *The New England journal of medicine*. 2018;378(2):113-25.
5. Creutz C, Tomsig J, Snyder S, Gautier M, Skouri F, Beisson J, et al. The copines, a novel class of C2 domain-containing, calcium-dependent, phospholipid-binding proteins conserved from Paramecium to humans. *The Journal of biological chemistry*. 1998;273(3):1393-402.
6. Lin H, Zhang X, Liao L, Yu T, Li J, Pan H, et al. CPNE3 promotes migration and invasion in non-small cell lung cancer by interacting with RACK1 via FAK signaling activation. *Journal of Cancer*. 2018;9(22):4215-22.
7. Tomsig J, Creutz C. Copines: a ubiquitous family of Ca(2+)-dependent phospholipid-binding proteins. *Cellular and molecular life sciences : CMLS*. 2002;59(9):1467-77.

8. Whittaker C, Hynes R. Distribution and evolution of von Willebrand/integrin A domains: widely dispersed domains with roles in cell adhesion and elsewhere. *Molecular biology of the cell*. 2002;13(10):3369-87.
9. Nalefski E, Falke J. The C2 domain calcium-binding motif: structural and functional diversity. *Protein science : a publication of the Protein Society*. 1996;5(12):2375-90.
10. Tomsig J, Snyder S, Creutz C. Identification of targets for calcium signaling through the copine family of proteins. Characterization of a coiled-coil copine-binding motif. *The Journal of biological chemistry*. 2003;278(12):10048-54.
11. Tang H, Zhu J, Du W, Liu S, Zeng Y, Ding Z, et al. CPNE1 is a target of miR-335-5p and plays an important role in the pathogenesis of non-small cell lung cancer. *Journal of experimental & clinical cancer research : CR*. 2018;37(1):131.
12. Heinrich C, Keller C, Boulay A, Vecchi M, Bianchi M, Sack R, et al. Copine-III interacts with ErbB2 and promotes tumor cell migration. *Oncogene*. 2010;29(11):1598-610.
13. Burk K, Ramachandran B, Ahmed S, Hurtado-Zavala J, Awasthi A, Benito E, et al. Regulation of Dendritic Spine Morphology in Hippocampal Neurons by Copine-6. *Cerebral cortex (New York, NY : 1991)*. 2018;28(4):1087-104.
14. Liang J, Zhang J, Ruan J, Mi Y, Hu Q, Wang Z, et al. CPNE1 Is a Useful Prognostic Marker and Is Associated with TNF Receptor-Associated Factor 2 (TRAF2) Expression in Prostate Cancer. *Medical science monitor : international medical journal of experimental and clinical research*. 2017;23:5504-14.
15. Jiang Z, Jiang J, Zhao B, Yang H, Wang Y, Guo S, et al. CPNE1 silencing inhibits the proliferation, invasion and migration of human osteosarcoma cells. *Oncology reports*. 2018;39(2):643-50.
16. Shao Z, Ma X, Zhang Y, Sun Y, Lv W, He K, et al. CPNE1 predicts poor prognosis and promotes tumorigenesis and radioresistance via the AKT signaling pathway in triple-negative breast cancer. *Molecular carcinogenesis*. 2020;59(5):533-44.
17. Cheal Yoo J, Park N, Lee B, Nashed A, Lee Y, Hwan Kim T, et al. 14-3-3 $\gamma$  regulates Copine1-mediated neuronal differentiation in HiB5 hippocampal progenitor cells. *Experimental cell research*. 2017;356(1):85-92.
18. Yoo J, Park N, Choi H, Park J, Yi G. JAB1 regulates CPNE1-related differentiation via direct binding to CPNE1 in HiB5 hippocampal progenitor cells. *Biochemical and biophysical research communications*. 2018;497(1):424-9.
19. Choi H, Park N, Lee B, Choe Y, Woo D, Park J, et al. CPNE1-mediated neuronal differentiation can be inhibited by HAX1 expression in HiB5 cells. *Biochemical and biophysical research communications*. 2020;533(3):319-24.
20. Liu S, Tang H, Zhu J, Ding H, Zeng Y, Du W, et al. High expression of Copine 1 promotes cell growth and metastasis in human lung adenocarcinoma. *International journal of oncology*. 2018;53(6):2369-78.
21. Du W, Liu T, Zhang Y, Zeng Y, Zhu J, Tang H, et al. MiR-195-5p is a Potential Factor Responsible for CPNE1 Differential Expression between Subtypes of Non-Small Cell Lung Cancer. *Journal of Cancer*. 2020;11(9):2610-20.
22. Yao W, Shan Z, Gu A, Fu M, Shi Z, Wen W. WW domain-mediated regulation and activation of E3 ubiquitin ligase Suppressor of Deltex. *The Journal of biological chemistry*. 2018;293(43):16697-708.
23. Zou X, Levy-Cohen G, Blank M. Molecular functions of NEDD4 E3 ubiquitin ligases in cancer. *Biochimica et biophysica acta*. 2015;1856(1):91-106.
24. Wang X, Duan J, Fu W, Yin Z, Sheng J, Lei Z, et al. Decreased expression of NEDD4L contributes to NSCLC progression and metastasis. *Biochemical and biophysical research communications*. 2019;513(2):398-404.
25. Gao S, Alarcón C, Sapkota G, Rahman S, Chen P, Goerner N, et al. Ubiquitin ligase Nedd4L targets activated Smad2/3 to limit TGF-beta signaling. *Molecular cell*. 2009;36(3):457-68.

26. Qu M, Han C, Srivastava A, Cui T, Zou N, Gao Z, et al. miR-93 promotes TGF- $\beta$ -induced epithelial-to-mesenchymal transition through downregulation of NEDD4L in lung cancer cells. *Tumour biology : the journal of the International Society for Oncodevelopmental Biology and Medicine*. 2016;37(4):5645-51.
27. Cui J, Shu C, Xu J, Chen D, Li J, Ding K, et al. JP1 suppresses proliferation and metastasis of melanoma through MEK1/2 mediated NEDD4L-SP1-Integrin  $\alpha\beta 3$  signaling. *Theranostics*. 2020;10(18):8036-50.
28. Sakashita H, Inoue H, Akamine S, Ishida T, Inase N, Shirao K, et al. Identification of the NEDD4L gene as a prognostic marker by integrated microarray analysis of copy number and gene expression profiling in non-small cell lung cancer. *Annals of surgical oncology*. 2013:S590-8.
29. Zhu J, Zeng Y, Li W, Qin H, Lei Z, Shen D, et al. CD73/NT5E is a target of miR-30a-5p and plays an important role in the pathogenesis of non-small cell lung cancer. *Molecular cancer*. 2017;16(1):34.
30. Yan Z, Wang Q, Lu Z, Sun X, Song P, Dang Y, et al. OSluca: An Interactive Web Server to Evaluate Prognostic Biomarkers for Lung Cancer. *Frontiers in genetics*. 2020;11:420.
31. Su Y, Gao C, Liu Y, Guo S, Wang A, Wang B, et al. Monoubiquitination of filamin B regulates vascular endothelial growth factor-mediated trafficking of histone deacetylase 7. *Molecular and cellular biology*. 2013;33(8):1546-60.
32. Fu S, Hu M, Peng Y, Fang H, Hsiao C, Chen T, et al. CUL4-DDB1-CRBN E3 Ubiquitin Ligase Regulates Proteostasis of ClC-2 Chloride Channels: Implication for Aldosteronism and Leukodystrophy. *Cells*. 2020;9(6).
33. Husnjak K, Dikic I. Ubiquitin-binding proteins: decoders of ubiquitin-mediated cellular functions. *Annual review of biochemistry*. 2012;81:291-322.

## Figures

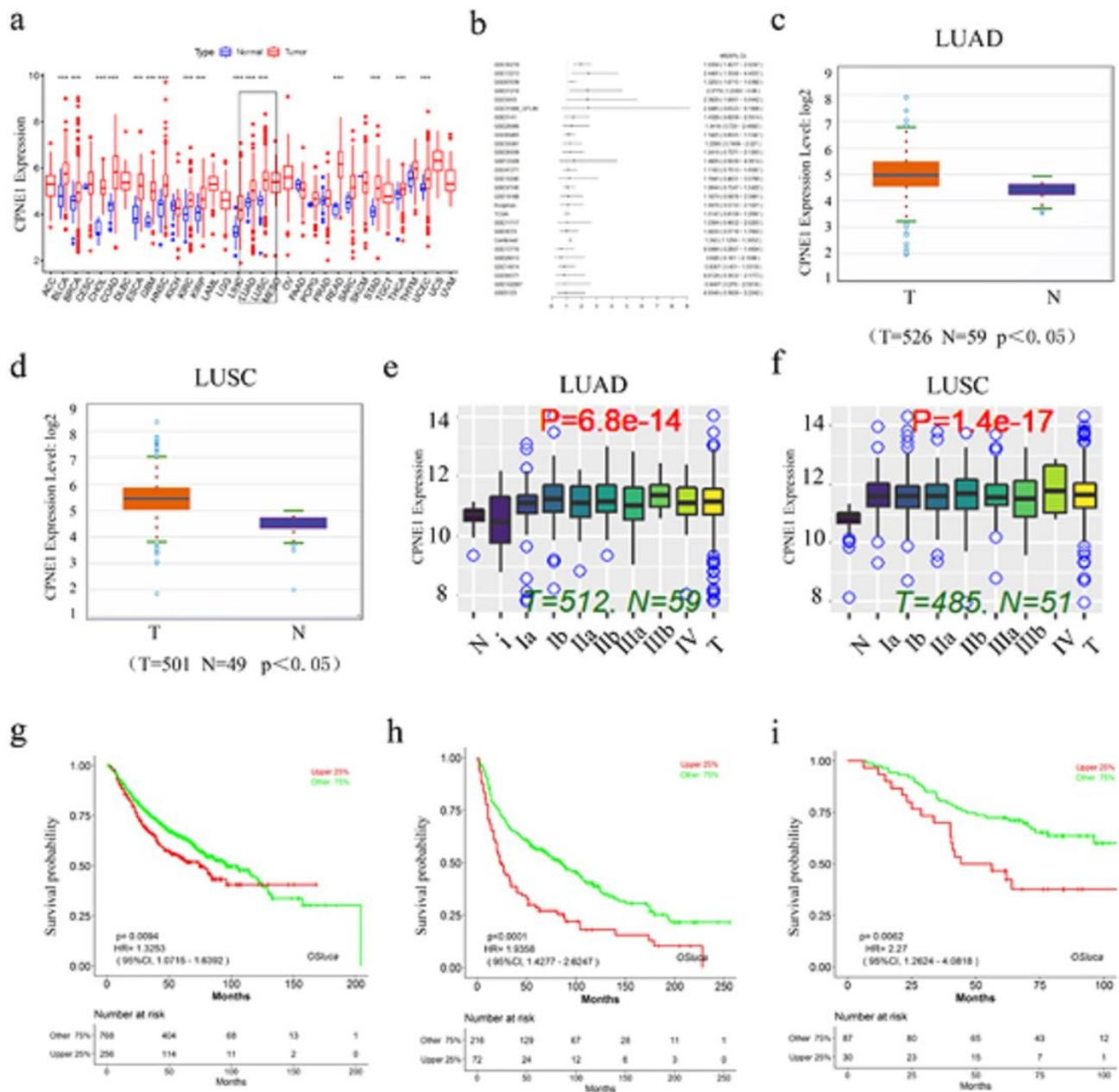


**Figure 1**

CPNE1 is elevated in lung cancer and correlates with poor survival a, b. CPNE1 is upregulated in a variety of cancers. c, d. CPNE1 is overexpressed in lung adenocarcinomas and lung squamous cell carcinoma. e, f. CPNE1 expression is correlated with the TNM stage of patients with lung adenocarcinoma/lung squamous cell carcinoma. g-i. CPNE1 expression is correlated with poor survival in lung adenocarcinoma/lung squamous cell carcinoma.

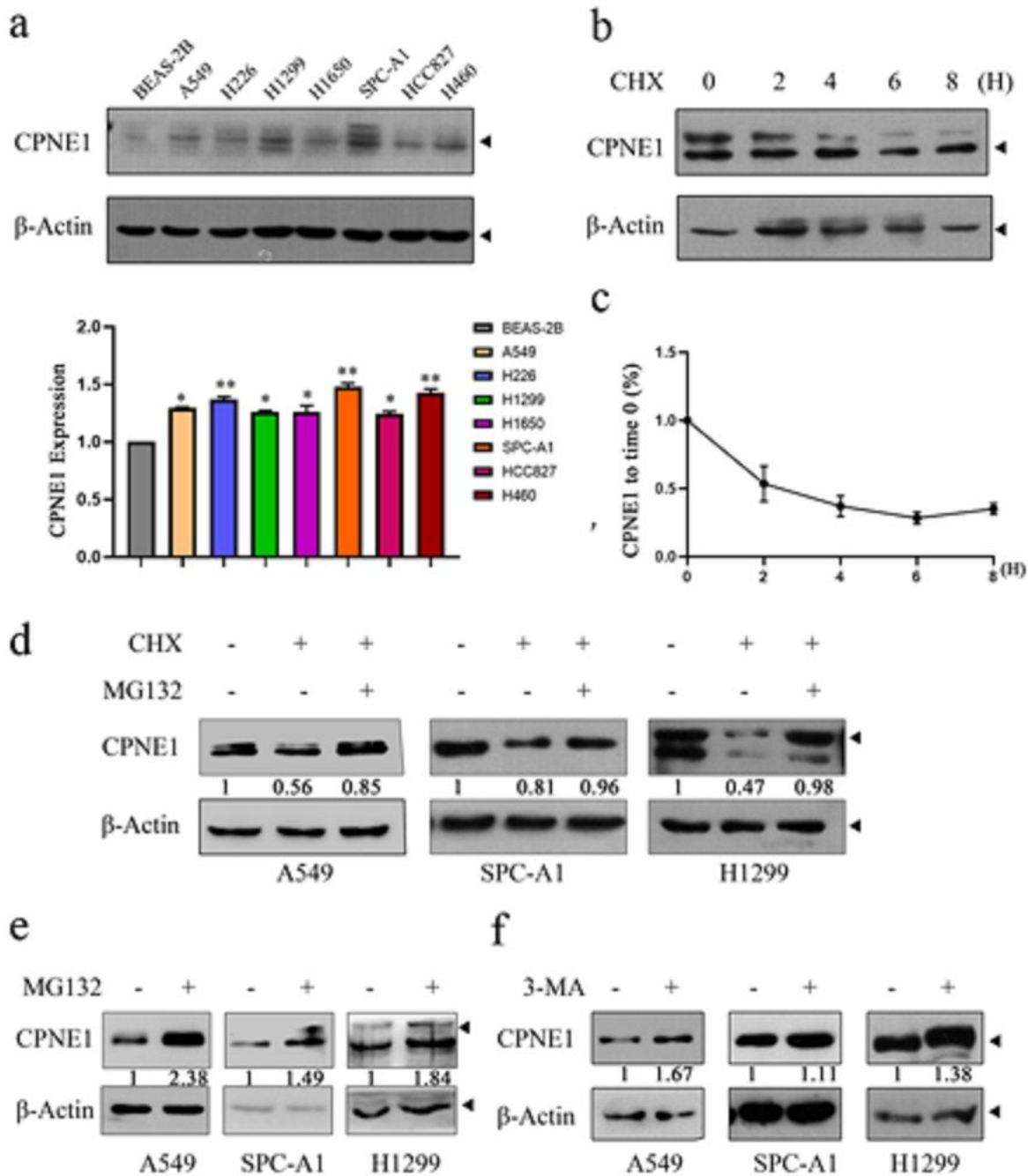


**Figure 2**

CPNE1 is degraded through both the ubiquitin-proteasome pathway and the autophagy-lysosome pathway. a. CPNE1 was highly expressed in lung cancer cell lines. b, c. CPNE1 was rapidly degraded in HEK293T cells. HEK293T cells were transfected with the Flag-CPNE1 plasmid and HA-Ub plasmid. After 48 h, cells were treated with 100  $\mu$ g/ml cycloheximide/vehicle for the indicated times. Cell lysates were prepared for Western blot analysis. The relative density of the CPNE1 band was measured with ImageJ software. d. The degradation of CPNE1 mediated by CHX was rescued by MG132. The indicated cell lines were seeded into six-well plates. After 24 h, cells were treated with 100  $\mu$ g/ml CHX or 100  $\mu$ g/ml CHX plus 10  $\mu$ M MG132 for 6 h. Cell lysates were prepared for Western blot analysis. e, f. Both MG132 and 3-MA can stabilize CPNE1. The indicated cell lines were seeded into six-well plates.

After 24 h, cells were treated with 10  $\mu$ M MG132 for 6 hours and 1 mM 3-MA for 18 h. Cell lysates were prepared for Western blot analysis.

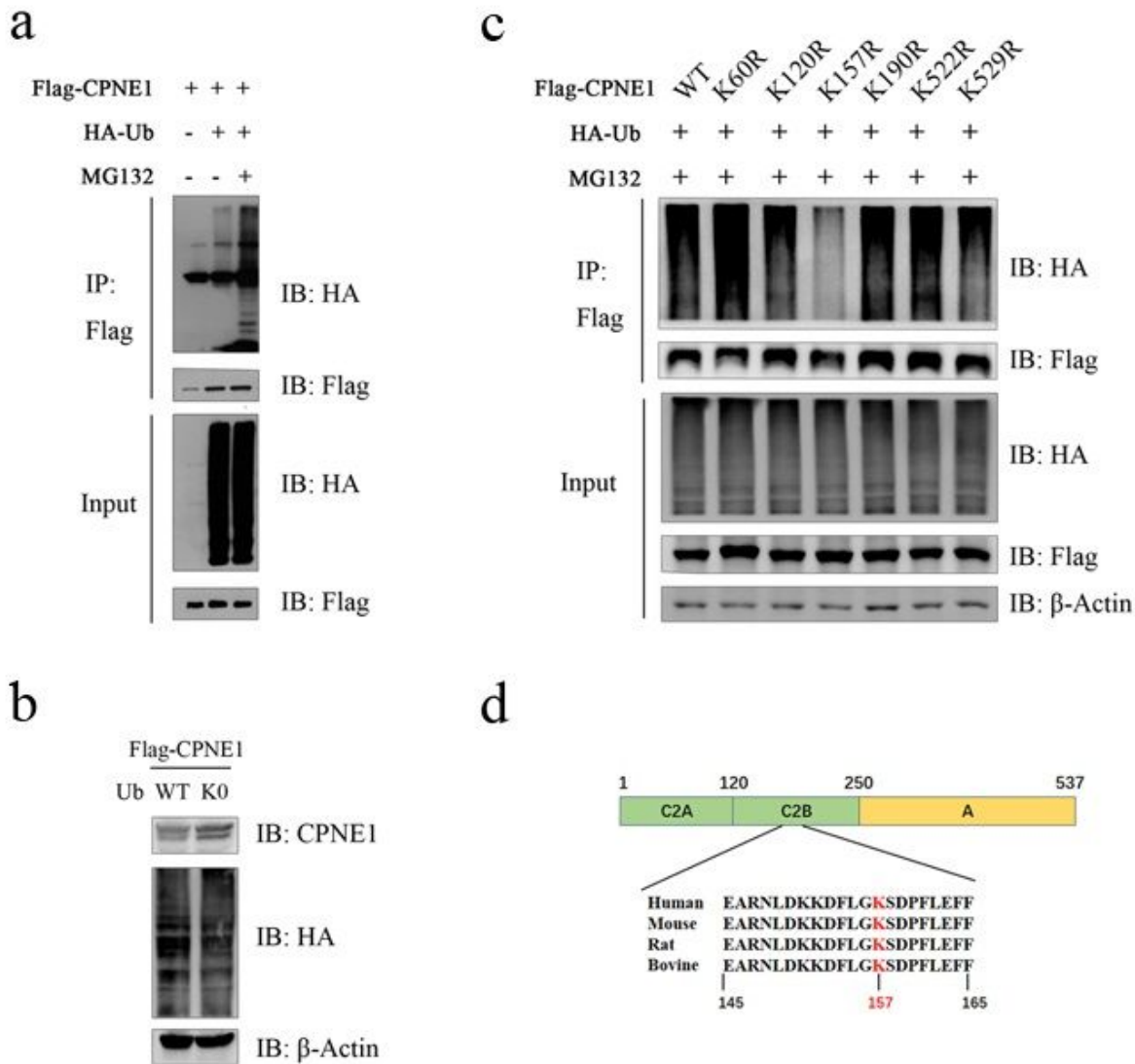


**Figure 3**

CPNE1 undergoes ubiquitination, and a highly conserved lysine at position 157 is subjected to ubiquitination. a. The co-IP assay confirmed the association between exogenous CPNE1 and Ub in HEK293T cells. HEK293T cells were transfected with 2  $\mu$ g of the Flag-CPNE1 plasmid and 2  $\mu$ g of the HA-Ub plasmid. After 24 h, cells were harvested with RIPA lysis buffer. Co-IP was performed as indicated. b. Co expression with Ub-K0 increased the expression of CPNE1. HEK293T cells were transfected with the Flag-CPNE1 plasmid and HA-Ub-WT/HA-Ub-K0 plasmids. Cell lysates were prepared for Western blot analysis. c. The K157 residue is the site of the interaction between CPNE1 and Ub. HEK293T cells were transfected with 2  $\mu$ g of the Flag-CPNE1-WT/mutant plasmids and 2  $\mu$ g of the HA-Ub plasmid. MG132 was added 2 h prior to cell harvesting. Co-IP was performed as indicated. d. The CPNE1 lysine 157 residue is conserved in many species, including humans, mice, rats, and bovines. The conserved lysine residue is indicated in red.

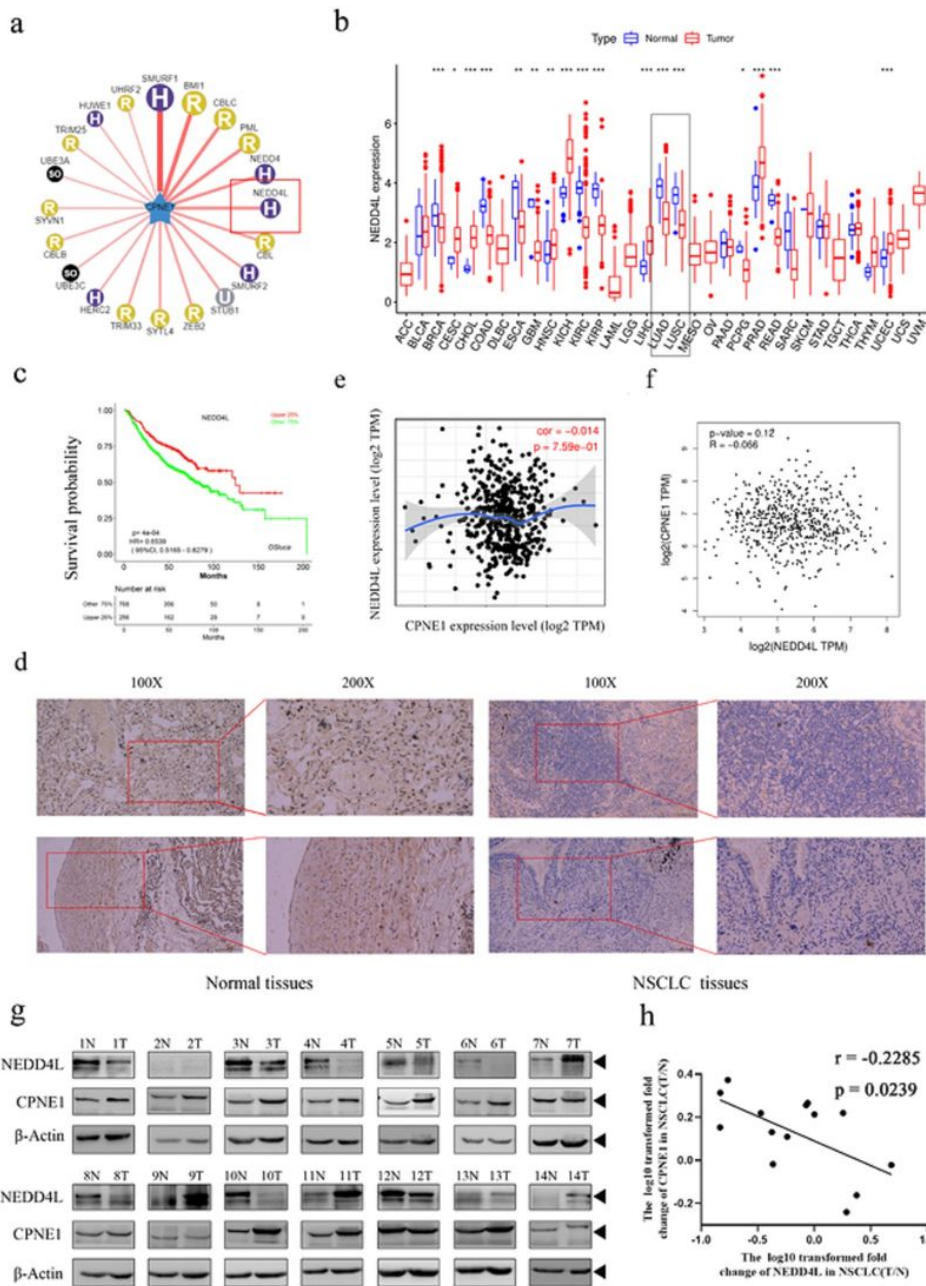


**Figure 4**

NEDD4L was identified as ubiquitin ligase for CPNE1 a. network view of the predicted E3 ligases for CPNE1 from Ubi-Browser. b. NEDD4L expression is downregulated in multiple types of human cancer. c. Low-level expression of NEDD4L is correlated with poor prognosis in lung cancer. d. Representative images of immunohistochemical staining for NEDD4L in lung adenocarcinoma tissues and normal tissues. e, f. The mRNA levels of CPNE1 and NEDD4L are unrelated in non-small cell lung cancer. g. Western blot analysis of CPNE1 and NEDD4L protein levels in 14 randomly selected NSCLC tissues and paired noncancerous lung tissues. The band density ratios represent the relative expression levels of CPNE1 and NEDD4L. h. Relative protein expression levels of CPNE1 and NEDD4L in 14 paired NSCLC tissues. The Y-axis indicates the log<sub>10</sub> transformed fold change in the T/N protein expression ratios of CPNE1 and NEDD4L. The number of each specimen is indicated below the X-axis.

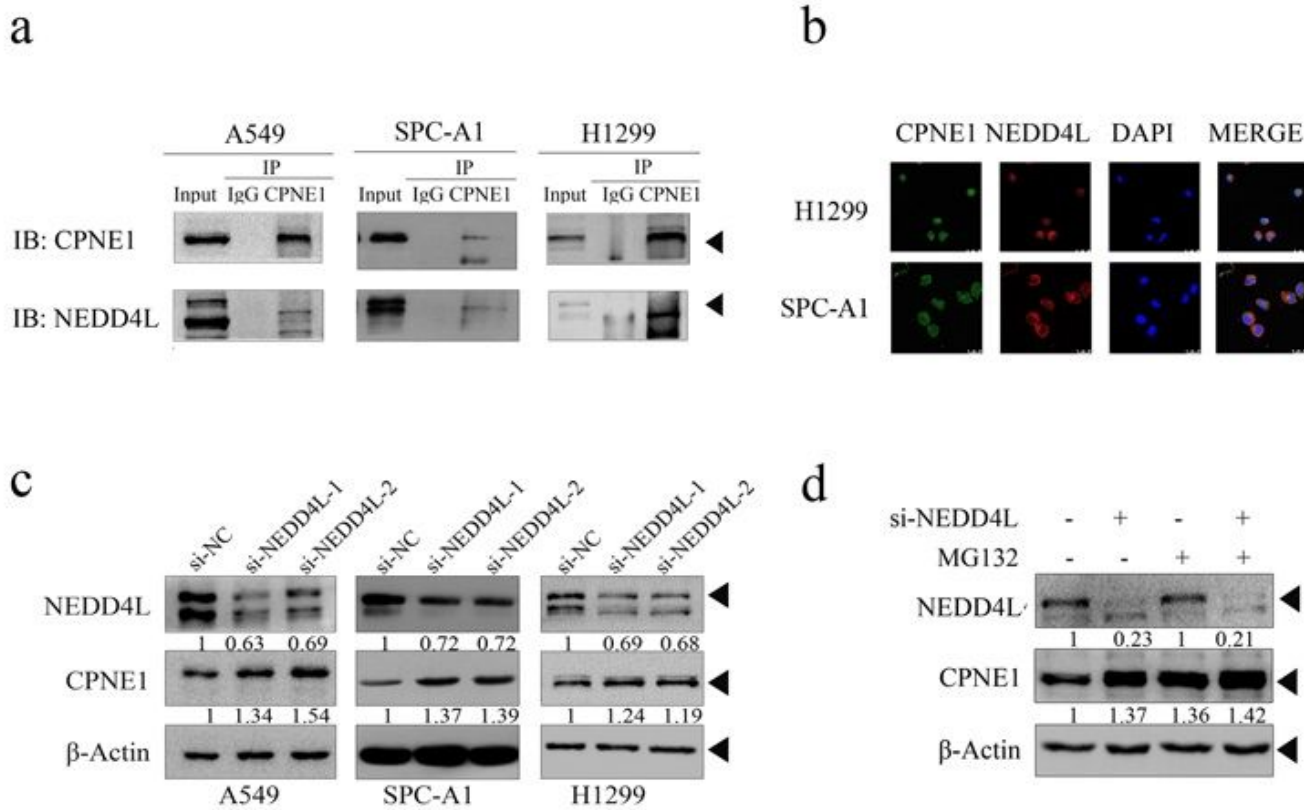


**Figure 5**

NEDD4L interacts with the CPNE1 protein. a. The co-immunoprecipitation assay proved the association between endogenous CPNE1 and NEDD4L. Co-immunoprecipitation was performed as indicated. b. Immunofluorescence was used to detect the intracellular localization of CPNE1 and NEDD4L. The intracellular localization of CPNE1 (green) and NEDD4L (red) is shown. c. CPNE1 protein levels in si-NEDD4L NSCLC cells. d. Upregulation of CPNE1 induced by NEDD4L interference was reduced by MG132 treatment. A549 cells were transfected with si-NEDD4L or si-Control. MG132 was added 6 h prior to protein extraction.

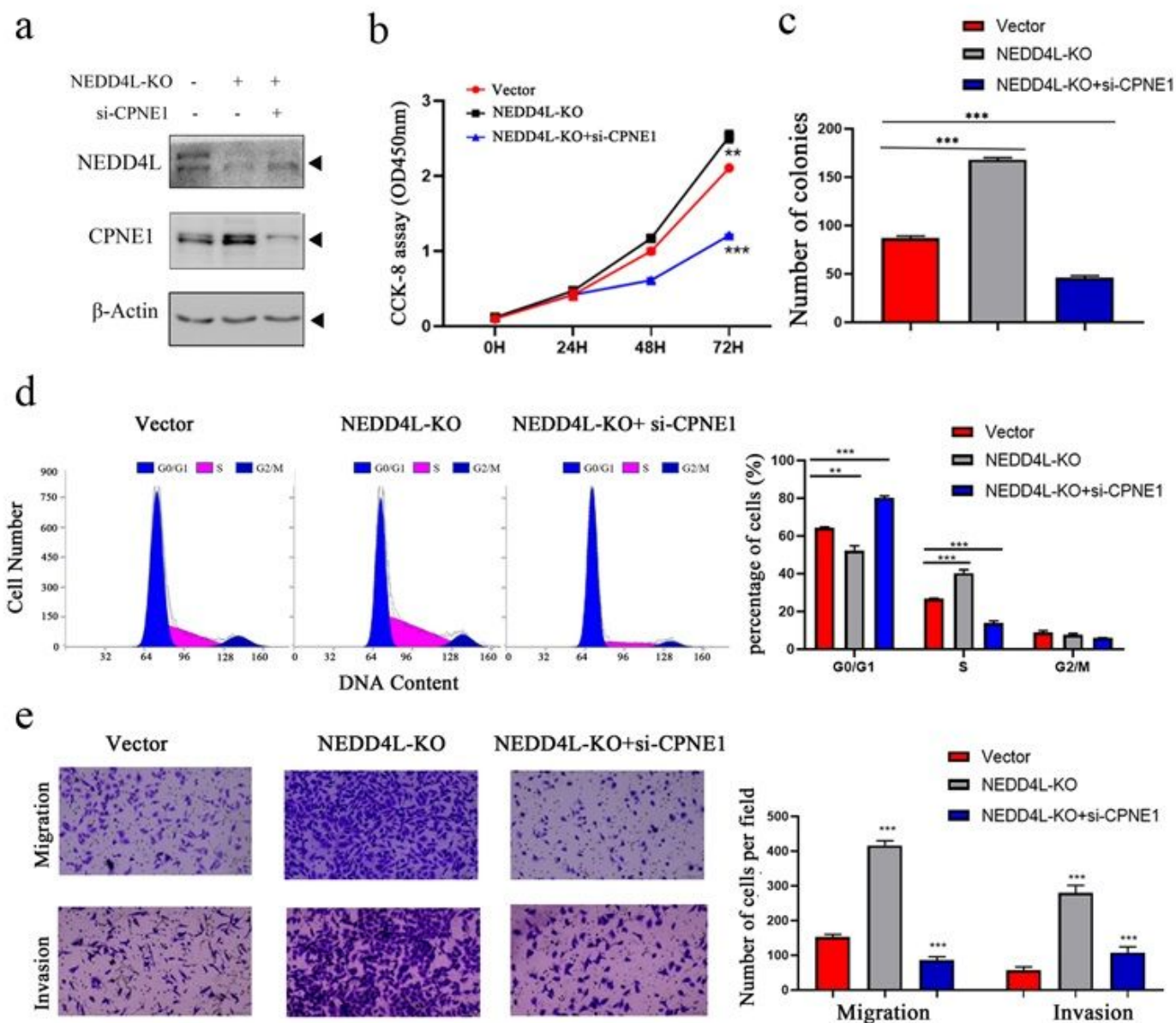


**Figure 6**

NEDD4L knockout promotes tumor cell proliferation and metastasis through CPNE1 a. CPNE1 protein levels in NEDD4L-KO/NEDD4L-KO NSCLC cells and NSCLC cells with CPNE1 interference. b. CCK-8 assay of cell viability in A549 cells. \* $P < 0.05$ ; \*\* $P < 0.01$ ; \*\*\* $P < 0.001$ . c. Representative images showing the results of clonogenic assays of cell proliferation in A549 cells. Bar charts showing the colony formation of cells. d. Flow cytometric assay of A549 cells. Cells were harvested 72 h after transfection and stained with PI. The percentage of cells in each cell cycle phase is shown in the inset of each panel. \* $P < 0.05$ ; \*\* $P < 0.01$ ; \*\*\* $P < 0.001$ . e. Representative images showing the results of transwell cell migration and invasion assays in A549 cells. \* $P < 0.05$ ; \*\* $P < 0.01$ ; \*\*\* $P < 0.001$ .

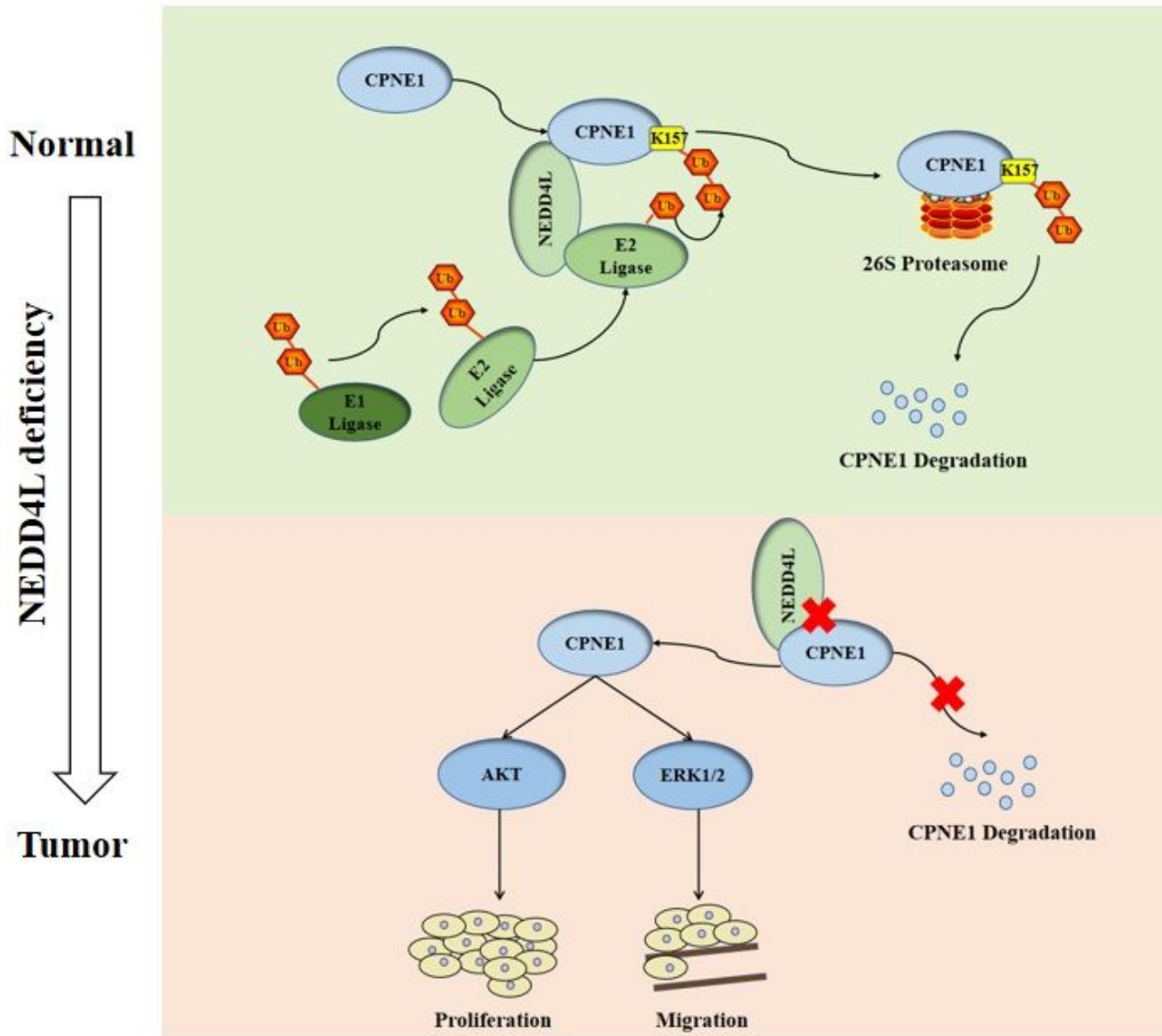


Figure 7

The hypothetical model for the functional interplay of CPNE1 with NEDD4L in non-small-cell lung cancer cells.

## Supplementary Files

This is a list of supplementary files associated with this preprint. Click to download.

- [SupplementaryTableS1.docx](#)
- [SupplementalTableS2.docx](#)
- [SupplementalTableS3.docx](#)
- [SupplementaryFig.1.docx](#)
- [SupplementaryFig.2.docx](#)